ARL-TR-9423 • MAY 2022

DEVCOM ARMY RESEARCH LABORATORY

Considerations for Casting Industrial-Scale Fe-Mn-Al-C Ingots

by Krista R Limmer, Daniel M Field, and Katherine M Sebeck

NOTICES

Disclaimers

The findings in this report are not to be construed as an official Department of the Army position unless so designated by other authorized documents.

Citation of manufacturer's or trade names does not constitute an official endorsement or approval of the use thereof.

Destroy this report when it is no longer needed. Do not return it to the originator.

ARL-TR-9423 ● MAY 2022

Considerations for Casting Industrial-Scale Fe-Mn-Al-C Ingots

Krista R Limmer and Daniel M Field
DEVCOM Army Research Laboratory

Katherine M Sebeck
DEVCOM Ground Vehicle Systems Center

REPORT DOCUMENTATION PAGE

Form Approved
OMB No. 0704-0188

1. REPORT DATE *(DD-MM-YYYY)*	2. REPORT TYPE	3. DATES COVERED (From - To)
May 2022	Technical Report	1 October 2016 – 10 January 2022

4. TITLE AND SUBTITLE
Considerations for Casting Industrial-Scale Fe-Mn-Al-C Ingots

5a. CONTRACT NUMBER

5b. GRANT NUMBER

5c. PROGRAM ELEMENT NUMBER

6. AUTHOR(S)
Krista R Limmer, Daniel M Field, and Katherine M Sebeck

5d. PROJECT NUMBER

5e. TASK NUMBER

5f. WORK UNIT NUMBER

7. PERFORMING ORGANIZATION NAME(S) AND ADDRESS(ES)
DEVCOM Army Research Laboratory
ATTN: FCDD-RLW-MF
Aberdeen Proving Ground, MD 21005

8. PERFORMING ORGANIZATION REPORT NUMBER
ARL-TR-9423

9. SPONSORING/MONITORING AGENCY NAME(S) AND ADDRESS(ES)

10. SPONSOR/MONITOR'S ACRONYM(S)

11. SPONSOR/MONITOR'S REPORT NUMBER(S)

12. DISTRIBUTION/AVAILABILITY STATEMENT
Approved for public release: distribution unlimited.

13. SUPPLEMENTARY NOTES
ORCID IDs: Krista R Limmer, 0000-0003-4775-5876; Daniel M Field, 0000-0002-8890-4391; Katherine M Sebeck, 0000-0001-6968-6512

14. ABSTRACT
When casting high-manganese, high-aluminum steels, the design of the casting molds and fluxes requires special consideration. Conventional low-alloy steel fluxes can react strongly with high-alloy content in the melt and cause variation in the resulting ingot composition. Casting mold size should also be considered due to segregation during solidification. This report reviews considerations for successful casting of industrial-scale ingots of high-manganese, high-aluminum steel alloys available in public domain literature.

15. SUBJECT TERMS
steel, ingot casting, Fe-Mn-Al-C, flux, teeming, Sciences of Extreme Materials

16. SECURITY CLASSIFICATION OF:			17. LIMITATION OF ABSTRACT	18. NUMBER OF PAGES	19a. NAME OF RESPONSIBLE PERSON
a. REPORT	b. ABSTRACT	c. THIS PAGE			Krista R Limmer
Unclassified	Unclassified	Unclassified	UU	23	19b. TELEPHONE NUMBER (Include area code) (410) 306-2039

Contents

List of Figures

List of Tables

1. Introduction

Iron-manganese-aluminum-carbon (Fe-Mn-Al-C) alloy steels have been identified as potential lightweight alternatives for rolled homogeneous armor (RHA) under MIL-DTL-12560[1] and cast homogeneous armor under MIL-A-11356[2] that would provide nearly identical armor-piercing ballistic performance at equivalent thicknesses. The production of these new armor materials would utilize existing infrastructure and manufacturing facilities to produce rolled plate such that a dimensionally constant material thickness, with lower structure weight, could be used anywhere RHA is employed.[3] Due to the high alloy content of Fe-Mn-Al-C alloys, domestic commercial scale-up of the manufacturing processes and ballistic test of wrought materials for either sheet or plate Fe-Mn-Al-C alloys has not previously been developed domestically.

The nominal composition range of Fe-Mn-Al-C alloys considered in this report has a Mn content ranging from 24 to 30 wt%, Al content from 7 to 10 wt%, C content from 0.8 to 1.1 wt%, with additions of up to 1 wt% silicon (Si), molybdenum (Mo), or vanadium (V), and a balance of Fe. This composition space, hereafter referred to as FeMnAl, is a subset of the patent application filed in 2017 by Howell et al.[4] Further claims in the patent space include casting the alloy to form a preform, heating the preform to a temperature in a range of about 1000–1200 °C, optional forging, and rolling the preform to form a steel plate. Heat treating of the produced plate includes solution treating between 900 and 1200 °C followed by water quenching and then aging the plate between 450 and 650 °C for up to 15 h in either a single- or two-stage aging treatment.

This report serves to collect the known considerations for successfully casting industrial-scale ingots of FeMnAl from a review of the available public domain literature. Specific lessons learned and best practices resulting from a series of industrial-scale melt and roll campaigns are documented elsewhere.[5]

2. Industrial Ingot Casting Process

Industrial-scale ingot casting generally includes two pouring operations: “tapping” is the initial transfer of the molten steel from the melt furnace to the ladle furnace for further refining and alloying, and “teeming” is the pouring of the liquid steel into the ingot molds. The optimum method for ingot casting is bottom pouring, where the molten steel is teemed from the ladle into a sprue and runner system that delivers molten steel to the bottom of one or more cast iron ingot molds arranged on a plate as shown in Fig. 1. Bottom pouring is preferred because it results in

higher-quality castings for two reasons: (1) reduced turbulence of the liquid steel and (2) the bottom of the ladle contains fewer nonmetallic impurities that typically float to the top compared to a top-pouring operation in which the steel is poured directly from the top of the ladle. During the teeming process, teeming fluxes are used to reduce or eliminate defects in the cast ingot, such as laps, ripple marks, entrapment of oxides, surface cracking, and pinhole porosity.[6]

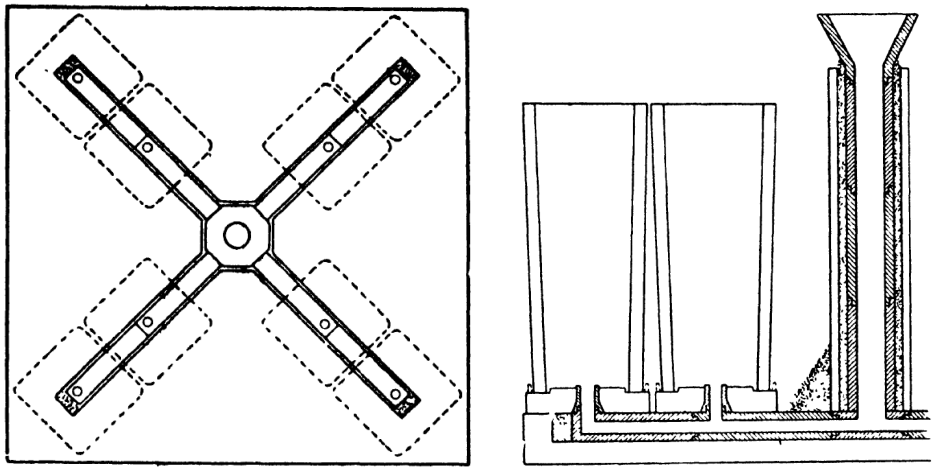

Fig. 1 Schematics of teeming through bottom pouring: top view of single trumpet feeding four runners (left) and side view of trumpet and one runner feeding two molds (right). (Reprinted from: Lister, W. Practical steelmaking. Chapman & Hall; 1929.)

In an industrial setting, teeming fluxes are suspended about a foot above the bottom of the mold before the teeming process begins. As the liquid steel enters the mold, the flux container is consumed and the flux powder is gently spread over the entire rising surface of the steel meniscus. The teeming flux is designed to have specific interactions with both the liquid and the solidified steel ingot. First, for the interaction with the liquid steel, the teeming flux provides an insulating layer to control solidification rate, a barrier to prevent re-oxidation of the steel, and a final refinement through adsorption or entrapment of inclusions to produce a cleaner casting. Second, the teeming flux also provides lubrication to isolate the solidified ingot from the mold and ensures uniform heat transfer between the steel and the mold. Mold fluxes developed for continuous casting applications have the same general functions, although the target viscosities and solidification rates are different. A more significant body of work has been published on mold fluxes than teeming fluxes due to the high volume of steel produced through continuous casting compared to ingot production. Continuous casting fluxes are highly engineered because poor flux performance during continuous casting operations is significantly more catastrophic. Casting fluxes are specifically tailored for two

main purposes: (1) lubrication between mold wall and (2) proper heat conduction to the copper mold. Because of the limited contact time between the mold flux and the molten steel in continuous casting, the melt refining aspects are not a factor and this difference should be taken into account when considering applying a mold flux for a teeming flux application.

Fluxes are a complex mix of oxides, minerals, and carbonaceous materials. The three primary oxides in mold fluxes are usually silica (SiO_2), lime (CaO), and alumina (Al_2O_3). Other common oxides in fluxes include sodium oxide (Na_2O), magnesium oxide (MgO), lithium oxide (Li_2O), iron oxide (e.g., FeO, Fe_2O_3), and boron oxide (B_2O_3). Fluorite (CaF_2) and carbonaceous materials are also included in fluxes as they can significantly affect the viscosity by disrupting the glass network. Fluxes are only effective while liquid, and complex composition development is often performed to ensure the correct viscosity for the application is met. Because fluxes comprise glass formers, there is no single solidus temperature—rather a wider temperature range over which the viscosity increases. The rate of this viscosity increase has been characterized as the basicity. Basic fluxes are referred to as "short" as their viscosity decreases rapidly as temperature decreases below the liquidus. Acidic fluxes ("long") have a wider fusibility range owing to their more gradual decrease in viscosity although they tend to be more viscous above the liquidus. Basicity is most simply defined as the ratio

$$B_1 = \frac{X_{CaO}}{X_{SiO_2}} \tag{1}$$

where X_i is the weight-percent of component i. A B-ratio of approximately 2 indicates acidic, a ratio of approximately 1 indicates basic, and a ratio of approximately 1.5 indicates neutral. More complex basicity equations can also be used for fluxes with large MgO or Al_2O_3 concentrations as seen in Eqs. 2 and 3.

$$B_2 = \frac{X_{CaO}+X_{MgO}}{X_{SiO_2}} \tag{2}$$

$$B_3 = \frac{X_{CaO}+X_{MgO}}{X_{SiO_2}+X_{Al_2O_3}} \tag{3}$$

High-basicity, low-viscosity fluxes are generally recommended for high-alloy steels, stainless steels, and high-C steels. This combination provides better thermal insulation and absorption of nonmetallic inclusions and is generally achieved through a combination of fluorides and alkali oxides. Fluxes for high-C steels should also have elevated C levels to prevent loss of C to the flux during teeming.

The thermal insulation properties of the teeming flux are critical to the macro segregation and defect formation in the ingot by influencing the solidification rate. Shrinkage during ingot solidification can lead to an internal defect known as "pipe,"

particularly in highly alloyed steels with long freezing ranges as shown in Fig. 2. One way to prevent pipe formation is through the use of a "hot top," which consists of side liners made of thermally insulating ceramics placed near the top of the ingot mold and an exothermic powder or board at the top end of the mold. The additional thermal insulation and heat input keep the steel at the top of the ingot molten longer allowing it to act as a reservoir and feed the ingot during the final solidification, preventing the pipe defect from forming. Additionally, the mold flux may either accelerate solidification through the continuation of endothermic reactions (heating, melting, and decomposition of the mold flux) causing increased heat losses, or it may decelerate solidification by the slag providing enhanced thermal insulation through the adsorption of radiation, which is dependent on the iron oxide (FeO) content. FeO, commonly found in fly-ash powders, provides more thermal insulation than Fe_2O_3, which reacts with C during melting. High-basicity fluxes with low iron contents, however, will crystallize leading to improved thermal insulation.[7]

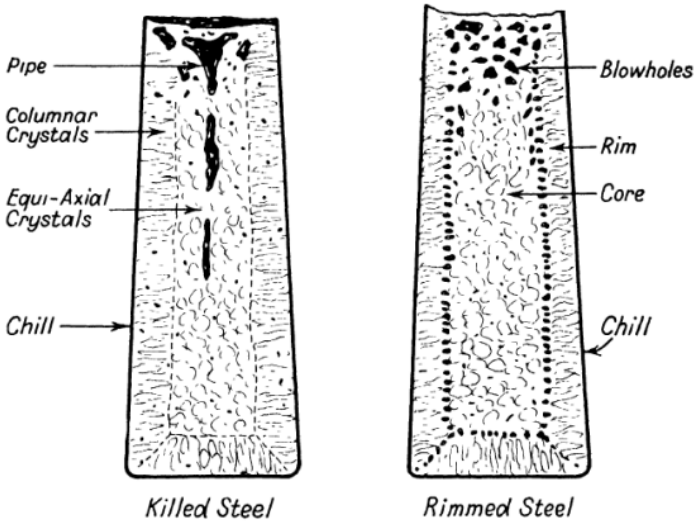

Fig. 2 Schematic of an ingot cross sections showing the presence of casting defects such as pipe and blowholes. (Reprinted from: Bashforth, GR. The manufacture of iron and steel. Vol. 2. Chapman & Hall; 1951.)

Other critical factors for ingot casting are the pouring temperature and rate. The pouring temperature is generally discussed in terms of "superheat," the difference between the liquidus (i.e., the temperature above which there is no solid) of the alloy and the pouring temperature. The superheat is a significant consideration in casting operations; if the superheat is too low, the fluidity and premature solidification of the molten metal are the primary concerns. Filling of the mold can be significantly impaired if the melt is not fluid enough, leading to the gating system

that feeds the mold from the downspout becoming clogged, thus preventing a mold from filling. Similarly, if the teeming temperature is too close to the liquidus (i.e., low superheat), the casting can begin solidifying during teeming leading to a similar problem of incomplete filling of the mold. Fluidity can be increased by increasing the temperature of the molten steel. However, if the superheat is too high, a variety of other problems can result: thermal erosion of the mold wall, casting defects, and segregation of alloying elements. In addition, given a lower vapor pressure associated with aluminum and manganese, excessive superheat can lead to alloying element losses. The most common casting defect caused by excessive superheat is excessive pipe, a phenomenon in which shrinkage defects start at the surface of the casting and burrow into the center of the casting as shown earlier in Fig. 2. Segregation of alloying elements can be caused by excessive superheat due to the increased time for solidification, leading to poor ingot quality and reduced homogeneity of the steel's behavior. Excessive superheat also increases the risk of oxide formation and increases interactions with the mold walls.

The pouring rate (or teeming rate) must also be controlled to balance between creating excessive turbulence when teeming too fast versus premature solidification before the mold has been filled. The teeming rate is controlled by the nozzle size, gating system, and number and size of molds arranged on a single plate. Turbulence in the molten steel can cause mold erosion and the formation of metal oxides that become entrapped in the casting. In a review of ingot casting practices, high-C steels are described as being teemed with a low superheat (40–45 °C) and high teeming rate (300 mm/min) to prevent severe segregation and subsequent crack formation, whereas stainless steels have both high superheat (60–70 °C) and high teeming rate (400 mm/min) to enable more inclusion floatation.[6] By comparison, the superheat used in laboratory-scale casting of Fe-Mn-Al-C steels is reported between 100 and 200 °C.[8] A larger superheat is used in the laboratory setting to prevent premature solidification from rapid thermal loss when working with a smaller ladle.

3. Flux Selection for Fe-Mn-Al-C Alloys

Over the past few decades there has been a surge in research and production of advanced high-strength steels with elevated Al content. The high-Al content in the molten steel strongly reacts with SiO_2 that is traditionally one of the main flux components. The SiO_2 content of the flux decreases over time and Al_2O_3 content increases due to the high affinity of the Al in the melt with oxygen as shown in the following reactions.[9]

$$4Al_{steel} + 3(SiO_2)_{slag} \leftrightarrow 2(Al_2O_3)_{slag} + 3Si_{steel} \quad (4)$$

$$2Mn_{steel} + (SiO_2)_{slag} \leftrightarrow 2(MnO)_{slag} + Si_{steel} \quad (5)$$

$$2Al_{steel} + 3(MnO)_{slag} \leftrightarrow (Al_2O_3)_{slag} + 3Mn_{steel} \quad (6)$$

Kim et al. performed a study looking at CaO-SiO_2-type flux interactions with Fe-Mn-Al-C steels and noted that elevated Al alloying content and elevated temperatures both led to an acceleration of the reactions, in good agreement with the rate-limiting step of this mechanism being the mass transfer of Al in the boundary layer.[10] One interesting note is the flux compositions published by POSCO for their Fe-Mn-Al-C alloys contain nontrivial amounts of SiO_2. Considering these as mold fluxes for continuous casting, the limited contact time between the flux and the molten steel limits SiO_2-Al_2O_3 interactions at the mold interface. The POSCO alloys also generally have lower Al-content, which further reduces SiO_2 interaction. An additional consideration is the open publication of these fluxes because of their failings, with the successful flux compositions safeguarded as corporate intellectual property.

In light of the problematic SiO_2 interactions with high-Al steels, a recent review of flux development for high-Al steels described CaO-Al_2O_3-based fluxes as the prevailing solution.[11] Of significant consideration has been the CaO/Al_2O_3 ratio, or C/A ratio, which has been evaluated over the range of 0.6–3.6 for continuous casting operations, as reported by Blazek et al. from ArcelorMittal.[12,13] The ideal C/A ratio is still under debate but in practice has been recommended to be approximately 1, where there is a minima in the liquidus temperature of the CaF_2-CaO-Al_2O_3.

Other oxide additions to the fluxes for high-Al alloys have included MnO to provide basicity control and alkali oxides (R_2O) such as Li_2O and Na_2O as viscosity and melt temperature modifiers. The Mn content of the alloys considered in the literature is significantly lower than FeMnAl, ranging from 0.2 to 1.5 wt%. No published work has been seen to systematically evaluate the effect of magnesium oxide (MgO), iron oxide (Fe_2O_3), or C-flux additions in the context of high-Al steels. The inclusion of borate (B_2O_3) has had mixed results in the continuous casting environment—decreasing viscosity and melting temperature but also reducing Al at high enough Al concentrations. Following an initial plant trial, it was decided to remove B_2O_3.[14]

A summary of published relevant alloys and fluxes trialed along with their outcomes is provided in the Appendix.

4. Alloying Considerations

The fluidity of Fe-Mn-Al-C alloys is generally improved by alloying additions such as Si, which is typical for most steel compositions. Laboratory-scale casting studies have shown that adding Si to Fe-Mn-Al-C alloys increases the fluidity and decreases both the liquidus and solidus temperatures, enabling casting with higher superheats without significantly raising the operating temperature.[15] The addition of 1 wt% Si has also been shown to minimize ferrite content and prevent deleterious formation of β-Mn during age hardening, with a suggested range of Si between 0.82% and 1.36% for optimization of castability, strength ductility, impact toughness, and age hardening.[8]

As with all high-performance alloys, the impurity content should be minimized during production of Fe-Mn-Al-C alloys. Sulfur (S), phosphorous (P), nitrides, and oxides are deleterious, significantly diminishing the impact toughness. The source of the Mn for the alloy has been shown to significantly affect the P content, with heats produced with ferromanganese containing 0.018–0.070 wt% P compared to 0.001–0.006 wt% P in heats produced with the more costly electrolytic manganese. Phosphorous levels as low as 0.018 wt% were shown to have a negative effect on the Charpy impact properties in cast FeMnAl. Electrolytic Mn is significantly more expensive than ferromanganese, but the resulting properties demand it be used. Another consideration in the use of electrolytic manganese is the temperature loss associated with melting large volume additions required to attain 30 wt% Mn. Ferromanganese is approximately 75% Mn, requiring a larger volume to be added than electrolytic Mn (99.9%). Finally, ferromanganese contains 6–7 wt% C, which must be accounted for along with other C-sources to avoid overshooting the targeted alloy C-content. POSCO has been able to circumvent all three of these concerns (phosphorous, carbon, and temperature loss) through infrastructure modifications to melt and refine ferromanganese in a second furnace, which is only cost effective when producing large amounts of high-Mn steels.

5. Conclusion

Industrial-scale casting of steel ingots uses a bottom-pouring method to increase casting soundness. During the bottom-pouring process, a teeming flux is also required to maximize casting cleanliness and prevent oxidation of molten steel surface as it rises in the mold. The design of fluxes for high-Mn and high-Al steels is relatively well documented in the public literature primarily as mold fluxes for continuous casting operations. Because mold fluxes perform slightly different functions than teeming fluxes, these results are not seamlessly transferable to ingot

casting operations. Further, optimal flux compositions are corporate intellectual property and are not generally disclosed. Other significant considerations during bottom pouring are the teeming temperature (superheat) and teeming rate. The teeming rate requires optimization of the nozzle diameter and number and size of the ingot molds located on each plate, which will vary depending on industrial capacity. One final general consideration for casting any steel is to keep the impurity content low. For high-Mn steels, this necessitates the use of electrolytic Mn because of the high-P content in ferromanganese.

6. References

1. MIL-DTL-12560K (MR) w/AMENDMENT 2. Armor plate, steel, wrought, homogenous (for use in combat-vehicles and for ammunition testing). CCDC Army Research Laboratory (US); 2019.

2. MIL-A-11356F. Armor, steel, cast, homogeneous, combat-vehicle type. Army Research Laboratory (US); 1987.

3. Howell RA, Gerth R. Fe-Mn-Al-C alloy steels - a new armor class. SAE International; 2017. SAE Technical Paper. doi:10.4271/2017-01-1703.

4. Howell RA, Cheeseman BA, Montgomery JS, Shirley AD, Sebeck K, Limmer K, inventors. High aluminum containing manganese steel and methods of preparing and using the same. United States patent 20190062881A1. 2019 Feb.

5. Limmer KR, Field DM, Sebeck KM, Kane J, DeGenova J, Thompson P, Schwartz D. Industrial-scale practice for casting Fe-Mn-Al-C ingots. DEVCOM Army Research Laboratory; 2022. Report No.: ARL-TR-9457.

6. Raja BVR. Selection of mould fluxes for production of high quality steel ingots. Steelworld. 2008;(December 2008):34–40.

7. Mills KC, Däcker CÅ. The casting powders book. Springer; 2017. doi:10.1007/978-3-319-53616-3

8. Howell RA. Microstructural influence on dynamic properties of age hardenable FeMnAl alloys [dissertation]. Missouri University of Science and Technology; 2009. https://scholarsmine.mst.edu/doctoral_dissertations/1940.

9. Bausch M, Frommeyer G, Hofmann H, Balichev E, Soler M, Didier M, Samek L. Ultra high-strength and ductile FeMnAlC light-weight steels. European Commission; 2013. doi:10.2777/33040.

10. Kim DJ, Park JH. Interfacial reaction between CaO-SiO 2-MgO-Al_2O_3 flux and Fe-xMn-yAl (x = 10 and 20 mass pct, y = 1, 3, and 6 mass pct) steel at 1873 K (1600 °C). Metall Mater Trans B. 2012;43(4):875–886. doi:10.1007/s11663-012-9667-x.

11. Wang W, Lu B, Xiao D. A review of mold flux development for the casting of high-Al steels. Metall Mater Trans B. 2016;47(1):384–389. doi:10.1007/s11663-015-0474-z.

12. Blazek K, Yin H, Skoczylas G, McClymonds M, Frazee M. Development and evaluation of lime-alumina based mold powders for casting high aluminum TRIP steel grades. AISTech - Iron and Steel Technology Conference Proceedings. 2011;8:1577–1586.

13. Cho J-WW, Blazek K, Frazee M, Yin H, Park JH, Moon S-WW. Assessment of $CaO–Al_2O_3$ based mold flux system for high aluminum TRIP casting. ISIJ Int. 2013;53(1):62–70. doi:10.2355/isijinternational.53.62.

14. Wu T, He S, Zhu L, Wang Q. Study on reaction performances and applications of mold flux for high-aluminum steel. Mater Trans. 2016;57(1):58–63. doi:10.2320/matertrans.M2015311.

15. Howell RA, Lekakh SN, Van Aken DC, Richards VL. The effect of silicon content on the fluidity and microstructure of Fe-Mn-Al-C alloys. Trans Am Foundry Soc. 2008;116(STEEL, Div 9-08-064):64–91.

16. Kim GH, Sohn I. Influence of Li_2O on the viscous behavior of $CaO–Al_2O_3$–12 mass% Na_2O–12 mass% CaF_2 based slags. ISIJ Int. 2012;52(1):68–73.

17. Li J, Shu Q, Hou X, Chou K. Effect of TiO_2 addition on crystallization characteristics of $CaO\text{-}Al_2O_3$-based mould fluxes for high Al steel casting. ISIJ Int. 2015;55(4):830–836.

18. Liu Q, Wen G, Li J, Fu X, Tang P, Li W. Development of mould fluxes based on lime–alumina slag system for casting high aluminium TRIP steel. Ironmaking Steelmaking. 2014;41(4):292–297.

19. Kim M-SS, Lee S-WW, Cho J-WW, Park M-SS, Lee H-GG, Kang Y-BB. A reaction between high Mn-High Al steel and CaO-SiO2-type molten mold flux: part I. Composition evolution in molten mold flux. Metall Mater Trans B. 2013;44(2):299–308. doi:10.1007/s11663-012-9770-z.

20. Wang Q, Sun M, Qiu S, Tian Z, Zhu G, Wang L, Zhao P. Study on mold slag with high Al_2O_3 content for high aluminum steel. Metall Mater Trans B. 2014;45(2):540–546. doi:10.1007/s11663-013-9929-2.

21. Yan W, McLean A, Yang Y, Chen W, Barati M. Evaluation of mold flux for continuous casting of high-aluminum steel. Advances in Molten Slags, Fluxes, and Salts: Proceedings of the 10th International Conference on Molten Slags, Fluxes and Salts. Springer; 2016. p. 279–289.

22. Yu X, Wen G, Tang P, Ma F, Wang H. Behavior of mold slag used for 20Mn23Al nonmagnetic steel during casting. J Iron Steel Res Int. 2011;18(1):20–25.

23. Zhao H, Wang W, Zhou L, Lu B, Kang YB. Effects of MnO on crystallization, melting, and heat transfer of CaO-Al_2O_3-based mold flux used for high Al-TRIP steel casting. Metall Mater Trans B. 2014. doi:10.1007/s11663-014-0043-x.

24. Shi C-B, Seo M-D, Cho J-W, Kim S-H. Crystallization characteristics of CaO-Al_2O_3-based mold flux and their effects on in-mold performance during high-aluminum TRIP steels continuous casting. Metall Mater Trans B. 2014;45(3):1081–1097.

Appendix. Review of Published Fe-Mn-Al-C Alloy Fluxes

Table A-1 Alloy compositions from relevant flux literature

ID	Ref	Mn	Al	Si	C	Other
A	[12]	…	…	…	…	high Al TRIP steel
B	[12]	…	…	…	…	high Al TRIP steel
C	[13]	…	…	…	…	1.45% Al TRIP Steel
D	[13]	…	…	…	…	1.45% Al TRIP Steel
E	[16]	…	…	…	…	none
F	[16]	…	…	…	…	none
G	[16]	…	…	…	…	none
H	[16]	…	…	…	…	none
I	[17]	…	…	…	…	none
J	[17]	…	…	…	…	none
K	[17]	…	…	…	…	none
L	[17]					none
M	[18]	1.386	0.9061	0.071	0.10	0.151 Mo
N	[19]	12.8–13.2	0.41–4.77	0.11–1.66	0.65	…
O	[19]	12.8–13.2	0.41–4.77	0.11–1.66	0.65	…
P	[19]	12.8–13.2	0.41–4.77	0.11–1.66	0.65	…
Q	[19]	12.8–13.2	0.41–4.77	0.11–1.66	0.65	…
R	[19]	12.8–13.2	0.41–4.77	0.11–1.66	0.65	…
S	[20]	21.5–25.0	1.5–2.5	<0.5	0.14–0.20	0.04–0.10 V
T	[20]	21.5–25.0	1.5–2.5	<0.5	0.14–0.20	0.04–0.10 V
U	[20]	21.5–25.0	1.5–2.5	<0.5	0.14–0.20	0.04–0.10 V
V	[14]	0.8	2.5	0.2	0.35	0.05 Ti, 0.02 Nb
W	[14]	0.8	2.5	0.2	0.35	0.05 Ti, 0.02 Nb
X	[14]	0.8	2.5	0.2	0.35	0.05 Ti, 0.02 Nb
Y	[14]	0.8	2.5	0.2	0.35	0.05 Ti, 0.02 Nb
Z	[14]	0.8	2.5	0.2	0.35	0.05 Ti, 0.02 Nb
AA	[21]	21.5–25.0	1.5–2.5	<0.5	0.14–0.20	0.04–0.10 V
BB	[21]	21.5–25.0	1.5–2.5	<0.5	0.14–0.20	0.04–0.10 V
CC	[21]	21.5–25.0	1.5–2.5	<0.5	0.14–0.20	0.04–0.10 V
DD	[21]	21.5–25.0	1.5–2.5	<0.5	0.14–0.20	0.04–0.10 V
EE	[21]	21.5–25.0	1.5–2.5	<0.5	0.14–0.20	0.04–0.10 V
FF	[21]	21.5–25.0	1.5–2.5	<0.5	0.14–0.20	0.04–0.10 V
GG	[21]	21.5–25.0	1.5–2.5	<0.5	0.14–0.20	0.04–0.10 V
HH	[21]	21.5–25.0	1.5–2.5	<0.5	0.14–0.20	0.04–0.10 V
II	[21]	21.5–25.0	1.5–2.5	<0.5	0.14–0.20	0.04–0.10 V
JJ	[21]	21.5–25.0	1.5–2.5	<0.5	0.14–0.20	0.04–0.10 V
KK	[21]	21.5–25.0	1.5–2.5	<0.5	0.14–0.20	0.04–0.10 V
LL	[22]	21.5–25.0	1.5–2.5	<0.5	0.14–0.20	0.04–0.10 V
MM	[23]	…	…	…	…	none
NN	[23]	…	…	…	…	none
OO	[23]	…	…	…	…	none
PP	[24]	…	…	…	…	POSCO 1.45 wt% Al steel
QQ	[24]	…	…	…	…	POSCO 1.45 wt% Al steel
RR	[24]	…	…	…	…	POSCO 1.45 wt% Al steel
SS	[24]	…	…	…	…	POSCO 1.45 wt% Al steel
TT	[24]	…	…	…	…	POSCO 1.45 wt% Al steel
UU	[24]	…	…	…	…	POSCO 1.45 wt% Al steel
VV	[24]	…	…	…	…	POSCO 1.45 wt% Al steel

Table A-2 Flux characteristics from relevant flux literature

ID	Ref	Type	Melting temperature (°C)	Crystallization temperature (°C)	Basicity (B_1)	Basicity (B_3)	C/A ratio
A	[12]	mold flux	1070	. . .	1.45	0.77	0.52
B	[12]	mold flux	905	. . .	1.97	1.83	1.70
C	[13]	mold flux	900	. . .	4.21	1.86	3.32
D	[13]	mold flux	875	. . .	4.25	1.85	3.29
E	[16]	initial mold slag	. . .	. . .	. . .	0.80	0.80
F	[16]	initial mold slag	. . .	. . .	. . .	0.80	0.80
G	[16]	initial mold slag	. . .	. . .	. . .	0.80	0.80
H	[16]	initial mold slag	. . .	. . .	. . .	0.80	0.80
I	[17]	mold flux	. . .	. . .	. . .	1.52	1.33
J	[17]	mold flux	. . .	. . .	. . .	1.41	1.31
K	[17]	mold flux	. . .	. . .	. . .	1.38	1.28
L	[17]	mold flux	. . .	. . .	. . .	1.42	1.31
M	[18]	mold flux	1164	. . .	8.04	1.11	1.00
N	[19]	mold flux	. . .	. . .	1.09	0.99	6.30
O	[19]	mold flux	. . .	. . .	0.32	0.33	2.96
P	[19]	mold flux	. . .	. . .	0.61	0.59	4.64
Q	[19]	mold flux	. . .	. . .	1.07	1.14	. . .
R	[19]	mold flux	. . .	. . .	1.09	0.84	2.80
S	[20]	initial mold slag	980	. . .	0.00	0.00	0.00
T	[20]	initial mold slag	1062	. . .	1.13	0.92	5.12
U	[20]	initial mold slag	921	. . .	0.99	0.93	17.95
V	[14]	mold flux	1001	. . .	1.67	0.91	1.90
W	[14]	mold flux	942	. . .	1.24	1.11	9.45
X	[14]	mold flux	1032	. . .	1.26	1.20	22.34
Y	[14]	mold flux	1155	. . .	7.95	1.35	1.53
Z	[14]	mold flux	1008	. . .	10.52	4.96	8.77
AA	[21]	mold flux	. . .	1205	4.13	0.52	0.60
BB	[21]	mold flux	. . .	1125	5.76	0.92	1.10
CC	[21]	mold flux	. . .	1050	6.77	1.29	1.60
DD	[21]	mold flux	. . .	1140	7.56	1.70	2.20
EE	[21]	mold flux	. . .	1421	8.38	2.32	3.20
FF	[21]	mold flux	. . .	1125	5.76	0.92	1.10
GG	[21]	mold flux	. . .	1138	6.50	0.94	1.10
HH	[21]	mold flux	. . .	1109	6.80	0.94	1.10
II	[21]	mold flux	. . .	1150	7.22	0.95	1.10
JJ	[21]	mold flux	. . .	1136	7.34	0.96	1.10
KK	[21]	mold flux	. . .	1177	7.86	0.97	1.10
LL	[22]	initial mold slag	964	. . .	0.30	0.28	3.02
MM	[23]	mold flux	1256	1149	1.06	0.48	0.78
NN	[23]	mold flux	1324	1166	1.09	0.49	0.78
OO	[23]	mold flux	1378	1204	1.12	0.49	0.78
PP	[24]	mold flux	. . .	. . .	0.55	0.50	5.24
QQ	[24]	mold flux	. . .	. . .	0.55	0.52	12.87
RR	[24]	mold flux	. . .	. . .	13.95	1.12	1.22
SS	[24]	mold flux	. . .	. . .	13.91	1.12	1.22
TT	[24]	mold flux	. . .	. . .	4.21	1.86	3.32
UU	[24]	mold flux	. . .	. . .	3.58	1.71	3.28
VV	[24]	mold flux	. . .	. . .	4.25	1.85	3.29

Table A-3 Flux compositions from relevant flux literature in weight-percent

ID	Ref	SiO_2	CaO	Al_2O_3	Na_2O	MgO	CaF_2	F	B_2O_3	Other
A	[12]	11	15.9	30.4	15.4	15.9	. . .	. . .	. . .	1.2 Fe_2O_3
B	[12]	9.8	19.35	11.4	14	19.35	. . .	. . .	15.9	1.3 Fe_2O_3
C	[13]	9	37.9	11.4	9	. . .	. . .	8.9	16	. . .
D	[13]	8.9	37.8	11.5	1	. . .	. . .	8.1	15	. . .
E	[16]	. . .	33.78	42.22	12	. . .	12	. . .	. . .	. . .
F	[16]	. . .	33.33	41.67	12	. . .	12	. . .	. . .	1 Li_2O
G	[16]	. . .	32.89	41.11	12	. . .	12	. . .	. . .	2 Li_2O
H	[16]	. . .	32	40	12	. . .	12	. . .	. . .	4 Li_2O
I	[17]	. . .	39.2	29.4	6.3	5.5	13.5	. . .	. . .	5.5 Li_2O
J	[17]	. . .	41	31.2	6.8	2.9	12.9	. . .	. . .	5 TiO_2, 5 Li_2O
K	[17]	. . .	35.2	27.6	6.5	2.9	13.3	. . .	. . .	7.5 TiO_2, 4.8 Li_2O
L	[17]	. . .	36.1	27.5	6.7	2.9	12.9	. . .	. . .	10 TiO_2, 4.8 Li_2O
M	[18]	3.5	28.15	28.15	13.6	7	. . .	7.4	10.3	1.8 Li_2O
N	[19]	33.6	36.53	5.8	13.8	2.5	. . .	7.6	. . .	. . .
O	[19]	53.5	16.9	5.7	13.8	2.5	. . .	7.6	. . .	. . .
P	[19]	43.7	26.7	5.76	13.8	2.35	. . .	7.6	. . .	. . .
Q	[19]	36.6	39	0	13.8	2.9	. . .	7.6	. . .	. . .
R	[19]	31.3	34	12.16	13.8	2.37	. . .	7.6	. . .	. . .
S	[20]	5.11	. . .	30.99	14.29	. . .	11.33	. . .	8.34	. . .
T	[20]	29.92	33.76	6.6	. . .	. . .	. . .	7.52	. . .	2.74 MnO
U	[20]	40.1	39.5	2.2	. . .	. . .	. . .		. . .	2.45 MnO
V	[14]	18.01	30.02	15.77	2.46	0.58	. . .	11.65	6.18	17.2 BaO, 2.39 Li_2O, 0.64 Fe_2O_3
W	[14]	33.94	42.24	4.47	2.59	0.25	. . .	12.6	6.29	2.47 Li_2O, 0.46 Fe_2O_3
X	[14]	36.38	45.79	2.05	2.66	0.34	. . .	9.28	3.83	1.93 Li_2O_3, 0.67 Fe_2O_3
Y	[14]	5	39.74	26	0	2	. . .	10	4.5	15.0 BaO, 2.0 Li_2O
Z	[14]	5	52.59	6	10	2	. . .	9.9	18	1.0 Fe_2O_3
AA	[21]	5	20.6	34.4	10	. . .	20		10	. . .
BB	[21]	5	28.8	26.2	10	. . .	20		10	. . .
CC	[21]	5	33.8	21.2	10	. . .	20		10	. . .
DD	[21]	5	37.8	17.2	10	. . .	20		10	. . .
EE	[21]	5	41.9	13.1	10	. . .	20		10	. . .
FF	[21]	5	28.8	26.2	10	. . .	20		10	. . .
GG	[21]	5	32.5	29.5	10	. . .	13		10	. . .
HH	[21]	5	34	31	10	. . .	0		20	. . .
II	[21]	5	36.1	32.9	10	. . .	6		10	. . .
JJ	[21]	5	36.7	33.3	10	. . .	0		15	. . .
KK	[21]	5	39.3	35.7	10	. . .	0		10	. . .
LL	[22]	40.7	12.4	4.1	. . .	. . .	16.7		. . .	. . .
MM	[23]	20.29	21.44	27.49	12.24	1.55	. . .	11.73	. . .	2.28 Li_2O, 3 MnO
NN	[23]	20.29	22.05	28.28	12.24	1.55	. . .	11.73	. . .	2.28 Li_2O, 1.6 MnO
OO	[23]	20.29	22.76	29.17	12.24	1.55	. . .	11.73	. . .	2.28 Li_2O
PP	[24]	36.4	19.9	3.8	11.1	. . .	. . .	9.8	. . .	2.1 Li_2O, 6.6 MnO_2
QQ	[24]	35.4	19.3	1.5	10.5	. . .	. . .	9.3	. . .	3.0 Li_2O, 6.2 MnO_2, 3.5 ZrO_2
RR	[24]	2.2	30.7	25.1	12.3	. . .	. . .	15.1	5.4	3.1 Li_2O
SS	[24]	2.3	32	26.2	7.4	. . .	. . .	13.9	. . .	6.4 Li_2O
TT	[24]	9	37.9	11.4	9	. . .	. . .	8.9	16	4.9 Li_2O
UU	[24]	11.9	42.6	13	4.8	. . .	. . .	9.3	10.8	4.9 Li_2O
VV	[24]	8.9	37.8	11.5	1	. . .	. . .	8.1	15	6.2 Li_2O

List of Symbols, Abbreviations, and Acronyms

Al	aluminum
Al_2O_3	aluminum oxide, also known as alumina
B_2O_3	boron oxide
BaO	barium oxide
C	carbon
CaO	calcium oxide, also known as lime
Fe	iron
Fe_2O_3	iron oxide
Fe-Mn-Al-C	iron-manganese-aluminum-carbon
FeMnAl	Fe-based alloy with 24–30 wt% Mn, 7–10 wt% Al, 0.8–1.1 wt% C, and <1 wt% Si, Mo, V
Li_2O	lithium oxide
MgO	magnesium oxide
Mn	manganese
MnO	manganese oxide
Mo	molybdenum
Na_2O	sodium oxide
O	oxygen
P	phosphorous
RHA	rolled homogeneous armor
Si	silicon
SiO_2	silicon oxide, also known as silica
V	vanadium

1 (PDF) DEFENSE TECHNICAL INFORMATION CTR
DTIC OCA

1 (PDF) DEVCOM ARL
FCDD RLD DCI
TECH LIB

8 (PDF) DEVCOM ARL
FCDD RLW MD
B CHEESEMAN
K CHO
FCDD RLW MF
K DOHERTY
D FIELD
E HORWATH
K LIMMER
M WALOCK
FCDD RLW PE
J MONTGOMERY

4 (PDF) DEVCOM GVSC
A GAFNER
J HEADING
K SEBECK
K VIEAU

1 (PDF) US ARMY PEO GCS
R HOWELL

1 (PDF) US ARMY PM MBTS
R NICOL